Enzyme Ribonucleotide Reductase: Unraveling an Enigmatic Paradigm of Enzyme Inhibition by Furanone Derivatives

Nuno M. F. S. A. Cerqueira, Pedro A. Fernandes, and Maria J. Ramos*

REQUIMTE/Faculdade de Ciências do Porto, Rua Campo Alegre, 687, 4169-007 Porto - Portugal

Received: February 8, 2006; In Final Form: May 10, 2006

Several 2′-substituted-2′-deoxyribonucleotides are potent inactivators of the enzyme ribonucleotide reductase (RNR), by destroying the essential tyrosyl radical located in subunit R2 or/and covalently alkylating the subunit R1. In the absence of external reductants, the inactivation is achieved by alkylation of subunit R1 by a methylene-3(*2H)*-furanone. The furanone is generated in solution through degradation of a keto-deoxyribonucleotide intermediate, produced during the inhibitory mechanism of a wide group of 2′-substituted inhibitors, and is easily detected experimentally by UV spectroscopy. Interestingly, the same keto-deoxyribonucleotide is also a proposed intermediate of the normal substrate pathway, but by some unknown reason, it does not dissociate from the active site and does not inactivate the enzyme. Therefore, if the currently accepted mechanism for substrate reduction is correct, there must be some specific reason that makes such a reactive intermediate behave differently, not dissociating from the active site during substrate reduction. In this article, we propose to validate the current substrate mechanism by showing that the keto-deoxyribonucleotide dissociates from the active site only in the case of the inhibitors, and therefore, it corresponds to a viable intermediate in the substrate mechanism. Furthermore, we answer unexplained experimental observations that concern the predomination of the normal reduction mechanism over the abnormal ketone formation in the FdNDP and the release of F^-, either in the normal or in the abnormal turnover. For that purpose, we have investigated the interaction between the enzyme and this keto-deoxyribonucleotide generated from the normal substrate and from two widely studied representative inhibitors. A model containing 140 atoms was used to represent the desired structures. The results allowed us to conclude that the solvation free energy of the 2′-substituents, its influence inside the active site, and the charge transfer mechanism from a protein side chain to solution are the thermodynamic driving forces for the intermediate dissociation and subsequent RNR inhibition. Such charge transfer cannot be accomplished by the natural substrate, preventing its dissociation. These results elucidate a paradox which has been unexplained for more than 20 years and further validates both the proposed substrate and inhibition chemical mechanisms.

Introduction

Ribonucleotide reductase (RNR) is a radical enzyme that is responsible for the reduction of ribonucleotides into deoxyribonucleotides (Scheme 1).[1,2] The knowledge that several processes within the cell are dependent on the concentration of deoxyribonucleotide, with some of them crucial for cell survival, such as DNA repair or DNA replication, made it one of the most studied enzymes in the past decade. This field is of present interest, since the correct knowledge of its machinery may allow the inducement of an externally programmed automatic cell destruction, which may be helpful in the treatment of several diseases such as cancer or AIDS.[3,4]

RNR is a ubiquitous enzyme, being expressed in a wide variety of organisms.[5] Although there are three different classes of RNR, they have a common radical-based reaction mechanism but with different amino acid sequences and different metallic cofactors.[6,7] Their classification into three classes is based on the metallic cofactor that is required to initiate the radical-dependent nucleotide reduction process.[8−10] *E. coli* class Ia ribonucleotide diphosphate reductase is one of the most characterized and investigated enzymes, since it serves as a prototype for the mammalian protein.

SCHEME 1: Ribonucleotide Reduction Catalyzed by RNR

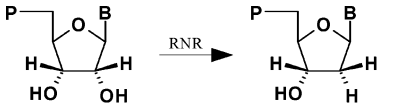

Ribonucleotides (1) Deoxyribonucleotides (2)

This enzyme was shown to be composed of a complex of two subunits from which the enzymatic activity is dependent. One of the subunits, named R1, controls the overall enzyme activity and is composed of two identical monomers, each lodging one active site containing five conserved residues, Cys225, Asn437, Glu441, Cys439, and Cys462, and three independent allosteric sites, named s-site, a-site, and h-site. The other subunit, named R2, is also composed of two identical monomers, each containing a stable neutral tyrosyl free radical coupled to a binuclear iron cluster that is required for its generation.

Recent studies with mRNR have shown that the RNR can be remarkably manipulated by a complex allosteric control system. It has been shown that it may be active in two different forms, as a dimer $R1_2R2_2$ and as a hexamer $R1_6R2_6$, with the

* Corresponding author. mjramos@fc.up.pt. Fax: 351-22-6082959.

10.1021/jp0608269 CCC: $33.50
Published on Web 09/30/2006

last one believed to be the major active form in the cytosol of normal cells in vivo.[11,12]

The reduction mechanism for this type of enzyme has been extensively studied during the past decade through X-ray crystallography, site-directed mutagenic experiments,[13−15] isotopic labeling and kinetics,[16,17] spectroscopic measurements,[18,19] small organic model approaches,[20,21] and theoretical calculations.[22−26] Many of the experimental studies involved substrate analogues that were able to preclude certain reaction steps of the mechanism. These results allowed the gathering of crucial information that helped to enlight the reduction pathway. At the same time, as some of these molecules behave as potent RNR inhibitors that preclude the formation of deoxyribonucleotides, they started to be developed and tested in vitro and in vivo as inducers of cell apoptosis.[27,28]

One of the first inhibitors that was able to inactivate RNR dates from 1976 and was developed by Thelander et al.[29] The inhibitor was a substrate analogue substituted at 2′-OH by a chlorine atom (*Cl*UDP). The experimental work showed that during the inactivation there was a measurable stoicheometric increase in the concentrations of uracil, inorganic pyrophosphate, and Cl^- in solution. By UV−visible spectroscopy, an interesting increase in the protein absorbance near 320 nm could also be seen.

Several inhibitors based on the substitution of the 2′-OH group, such as 2′,2′-difluoro-2′-deoxycytidine-5-diphosphate (F_2dNDP or as usually called gemcitabine), 2′-deoxy-2′-methylenenucleoside-5′-diphosphate (CH_2dNDP),[30] 2′-azido-2′-deoxynucleoside-5-diphosphate (N_3dNDP),[29] (*E*)-2′-fluoromethylene-2′-deoxycytidine-5-diphosphate (*CHF*dNDP),[31,32] or 2′-mercapto-2′-deoxycytidine-5-diphosphate (*SH*dNDP),[33] turned up in the preceding years with very interesting inhibitory properties. From these, N_3dNDP, F_2dNDP, and *CHF*dNDP are the most interesting ones due to the potent antitumor efficacy against a wide range of tumors (Table 1).[34,35] The success of some of these inhibitors in clinical trials, such as *CHF*dNDP or gemcitabine, have already promoted their approval by drug agencies in the treatment of certain kind of tumors, such as nonsmall cell lung cancer, adenocarcinoma of pancreas, and bladder cancer.

Experimental studies with many of these inhibitors have shown several similarities with *Cl*UDP.[36] With the exception of CH_2dNDP[30] and *CHF*dNDP, all 2′-substrate analogues undergo the release of the substituents attached to carbon C-2′ of the ribose ring, the cleavage of the base from the sugar moiety, the release of inorganic pyrophosphate, and in most of cases an increase of the absorption band around the 320 nm.[37−39]

These interesting features earned the attention of researchers, especially the nature of the characteristic absorption band at 320 nm that is common in most of the inhibitors (Table 1). This signal was shown to be linked with the formation of a complex between the protein and a furanone derivative **5** (2-methylene-3(*2H*)-furanone) (Scheme 2)**.** The furanone is the degradation product of a ketone (**4**), which is an intermediate product of the inhibitory mechanism and is able to dissociate from the active site. In the absence of reductants such as thioredoxin, dithiothreitol (DTT), or glutathione,[40,41] the furanone derivative inhibits RNR by Michael addition/alkylation, probably on a lysine residue of subunit R1, giving rise to the characteristic absorption band at 320 nm (Scheme 2).[37]

With some mutagenic experiments taken into account, this ketone intermediate is believed to be a degradation product of a keto-deoxyribonucloetide **4**—the product of the second step of several proposed inhibitory mechanisms.

TABLE 1: RNR Substrate Analogues and Furanone Derivatives Detected during the Inhibitory Mechanism

Inhibitors	Inhibitor Structure	Furanone Derivative	UV/Vis
*F*dNDP	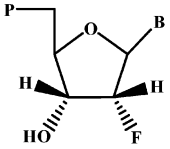	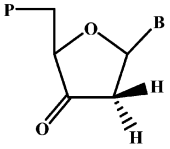	320 nm
*Cl*dNDP	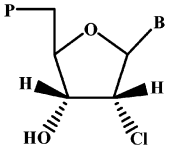	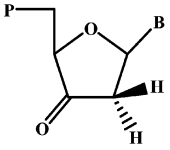	320 nm
N_3dNDP	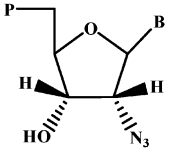	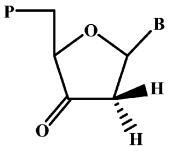	320 nm
F_2dNDP	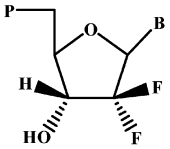	-	-
*SH*dNDP	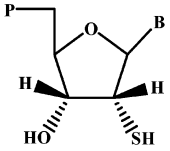	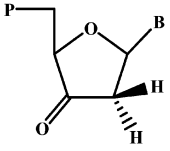	320nm*
*CHF*dNDP	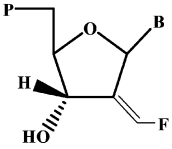	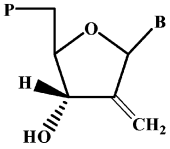	370nm

*The formation of the keto-deoxyribonucleotide (the precursor of the furanone derivative) is theoretically predicted in the absence of molecular oxygen.[42] The experimental work is inconclusive.[33]

Interestingly, until the formation of the keto-deoxyribonucleotide, the proposed inhibitory mechanisms of the 2′-substrate analogues and the normal reduction pathway are very similar.[23,24,43] The first two steps are almost identical, and the only difference relates to the nature of the atom(s) that is (are) attached to carbon C-2′. Both mechanisms yield by the end of the second step a radical keto-deoxyribonucleotide **2**, that after the third step generates a common keto-deoxyribonucleotide, the most stable intermediate of the proposed RNR mechanisms.

The key difference between the normal turnover and the inhibitory mechanism occurs after the third step.[42,44−48] In the case of the natural substrate, it has been proposed that the ketone **3** undergoes a proton-coupled electron transfer (CP-ET),[23] i.e., the migration of the acidic proton from Glu441 to the 3′ keto group of the keto-deoxyribonucleotide together with a simultaneous electron transfer from the radical anionic disulfide bridge to carbon C-3′ of the keto-deoxyribonucleotide. This reaction is then followed by a hydrogen atom transfer from Cys439 to carbon C-3′ of the substrate generating the deoxyribonucleotide **6**—the final product of the reduction process. In the case of the inhibitory mechanisms, ketone **4**, which is equivalent to ketone **3** in the normal reduction pathway (when $R^2 = H$), is unable to continue the normal reduction pathway and dissociates from the active site by an unknown reason. In solution, it undergoes elimination of the base and of the phosphate moiety to produce

SCHEME 2: Schematic Representation of the Normal Reduction Pathway and an Inhibitory Mechanism of RNR With Their Common Keto-Deoxyribonucleotide Intermediate

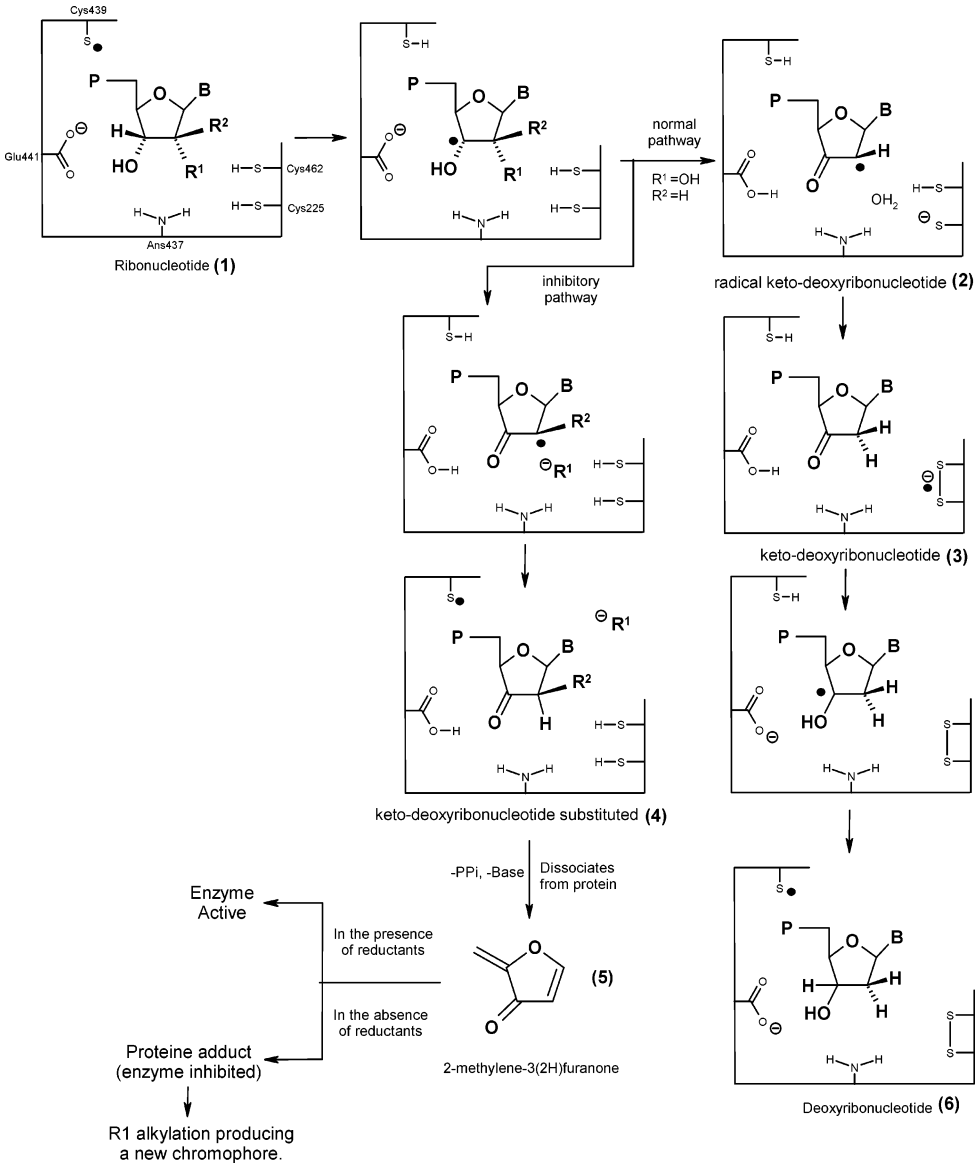

2-methylene-3(*2H*)-furanone (**5**). This furanone is thus meant to be responsible for enzyme inactivation by covalent addition with one of the monomers of subunit $R1_2$ giving rise to a characteristic absorption band.

Such unexplained and apparently contradictory behavior raises important questions regarding the reliability of the proposed substrate mechanism or/and inhibitory mechanism. At the same time, the cause (or causes) that allows, within some inhibitors, the release of the keto-deoxyribonucleotide from the active site into the solution are still unknown, contrary to what happens with the same species in the normal reduction pathway. This important question motivates the present study.

This article is focused on the evaluation of the dissociation energy between the enzyme and the keto-deoxyribonucleotide in three different situations. One situation corresponds to the fourth step of the catalytic mechanism of the natural substrate, where the keto-deoxyribonucleotide is formed but does not dissociate from the active site. The other two characterize the pre-steady-state before the dissociation of the keto-deoxyribonucleotide into the solution in two different inhibitors.

To accomplish this work, an extended model of the active site was used, including Cys439, Glu441, and Asn437 linked by a heptapeptide together with Cys225 and Cys462. This model can efficiently account for the restrained mobility of the reactive residues, as well as most of the long-range enzyme−substrate interactions, allowing a clear evaluation of the role of the enzyme as shown in our previous works.[25,26]

In the present study, the constructed model corresponds to the biggest model of RNR built and studied theoretically at the density functional theory (DFT) level.

Methodology

A. Modeling. The model system used in this work, for all the studied cases, was based on the crystal structure determined by Eriksson et al.,[49] in which the relevant residues were kept and the others deleted. The system includes all active site residues, Cys439, Glu441, Asn437, Cys225, and Cys462, and all residues within Ser436 and Ile442. The model was truncated at Ser436 and Ile442, with neighbor residues Gln435 and Ala443 replaced by hydrogens, resulting in neutral NH_2 and COH terminations, respectively. Cys225 and Cys462 were modeled as free methiothyol groups, because they are located at opposite sites of the heptapeptide. The inclusion of extra residues from

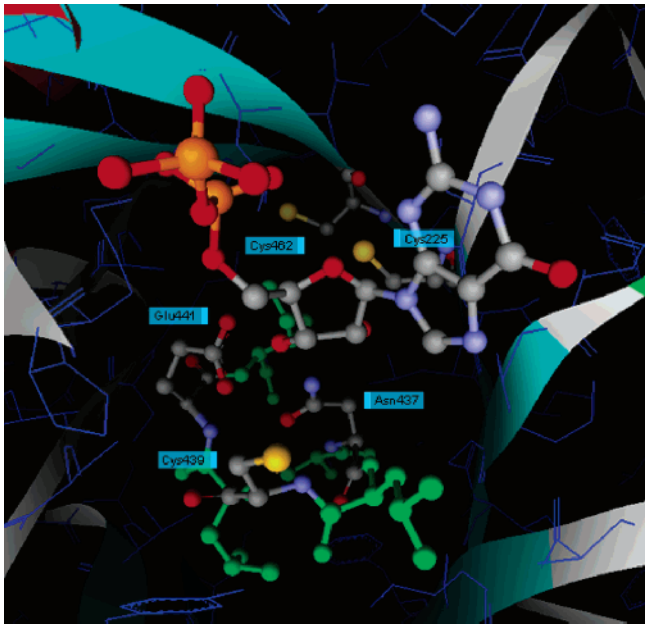

Figure 1. The model system built from the X-ray structure. The amino acids included in the computational model are shown in ball-and-stick representation. The region of R1 not included in the model is shown in dark blue.

Cys225 to Asn437 and from Glu441 to Cys462, to connect both cysteines to the heptapeptide, seemed unreasonable to us, since they will not significantly change the results and will only result in a big increase in the variables to be computed. Moreover, it is known that these cysteines have high mobility inside the active site, e.g., Cys462 can be distanced by ~9 Å from C-3′ of the substrate when both cysteines are in the reduced form or come closer by ~4 Å when both cysteines are oxidized to generate the radical anionic disulfide bridge.[49−51] The substrate was modeled without the phosphates and the base, which were replaced by hydrogens. Hydrogen atoms were added using InsightII.[52]

To carry out this study, we have modeled three different structures E:S:Lg that characterize the products of three reactions (Figure 1). One represents to the product of the fourth step of the reduction mechanism of the natural substrate. The other two systems correspond to the products of the fourth step of the inhibitory mechanism of *Cl*dNDP and *F*dNDP. In all cases, the substrate analogue is found to be a keto-deoxyribonucleotide but is surrounded by different environments promoted by the reactions of the preceding steps.[25,26,46]

Each system was then divided in two main regions (Figure 2, left). One corresponds to the enzyme, called enzyme region (E), and the other is named substrate region (S) that includes the substrate analogue—the keto-deoxyriblonucleotide.

In all studied reactions, after the second step of the mechanism, the dissociation of the atom(s) attached to C-2′ of the substrate occurs, and as it remains unbounded till the end of the reaction, we have also created another region named the Lg group (leaving group). In the normal reduction pathway, the Lg Group corresponds to a water molecule, and in the case of the inhibitors, it corresponds to an anionic fluorine or an anionic chlorine depending on the modeled reaction.

Subsequently, we used these models to create two more systems, E:S and E:Lg. The system E:S contains the enzyme and the substrate regions and the system E:Lg contains the enzyme region with the Lg group.

B. Geometry Optimizations. The overall system (E:S:Lg model) contains the substrate, the Lg group, and the heptatpeptide that connects Ser436 to Ile442 and two cysteines, Cys225 and Cys462, that were modeled as methiothyol groups. The resulting model contains a total of 140 atoms forming the largest system known in RNR that was treated at the DFT level. To deal with such a large system (140 atoms), we resorted to the ONIOM method as implemented in *Gaussian 03*, using it in all geometry optimizations. This method allows the division of the system into several regions, each one calculated with a different theoretical level.[53−57]

According to the ONIOM methodology, we have divided the system into two consecutive layers, designed as the high-level and low-level layers (Figure 2, right). The high-level layer includes the keto-deoxyribonucleotide (substrate region) without the phosphates and the base, the Lg group and all atoms that are closer to the substrate or the inhibitor (part of the enzyme region), i.e., the sulfur (radical or protonated), and the neighbor β-CH_2 of Cys439, the carboxylate group, and the neighbor β-CH_2 of Glu441, the amide group of Asn437, and both methylthiols groups that correspond to Cys225 and Cys462. The low-level layer contains the remaining atoms.

The atoms included in the high-level layer are those that undergo more significant geometric rearrangements during the

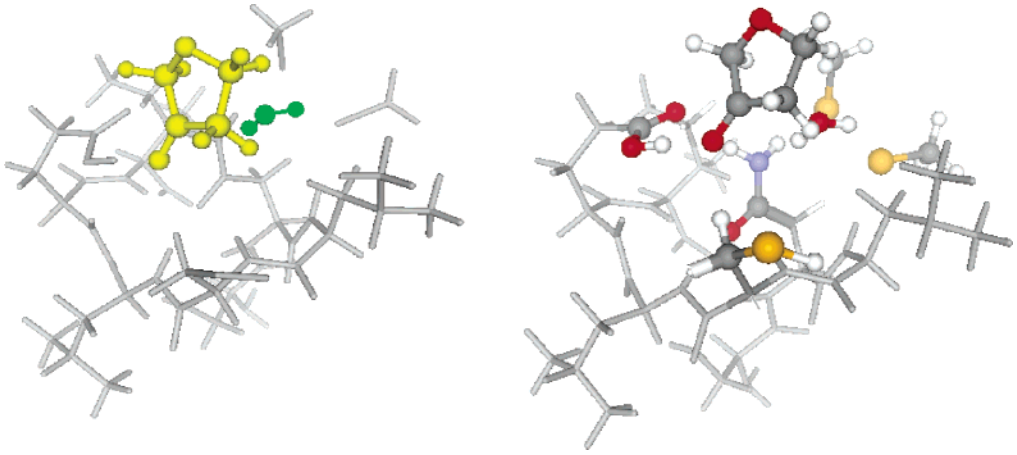

Figure 2. Left: the S, Lg, and E models of the E:S:Lg model for each system (taking as example the minimum of the normal reduction mechanism). The S model is represented in ball-and-stick and colored yellow; the Lg model is represented also in ball-and-stick but colored green; and the remaining part corresponds to the E model and is shown in stick representation and colored in gray. Right: the high-level and low-level layers division of the E:S:Lg model used in each system during the geometry optimizations with the ONIOM method. The high-level region is represented in ball-and-stick, and the lower-level region is represented in stick colored in gray.

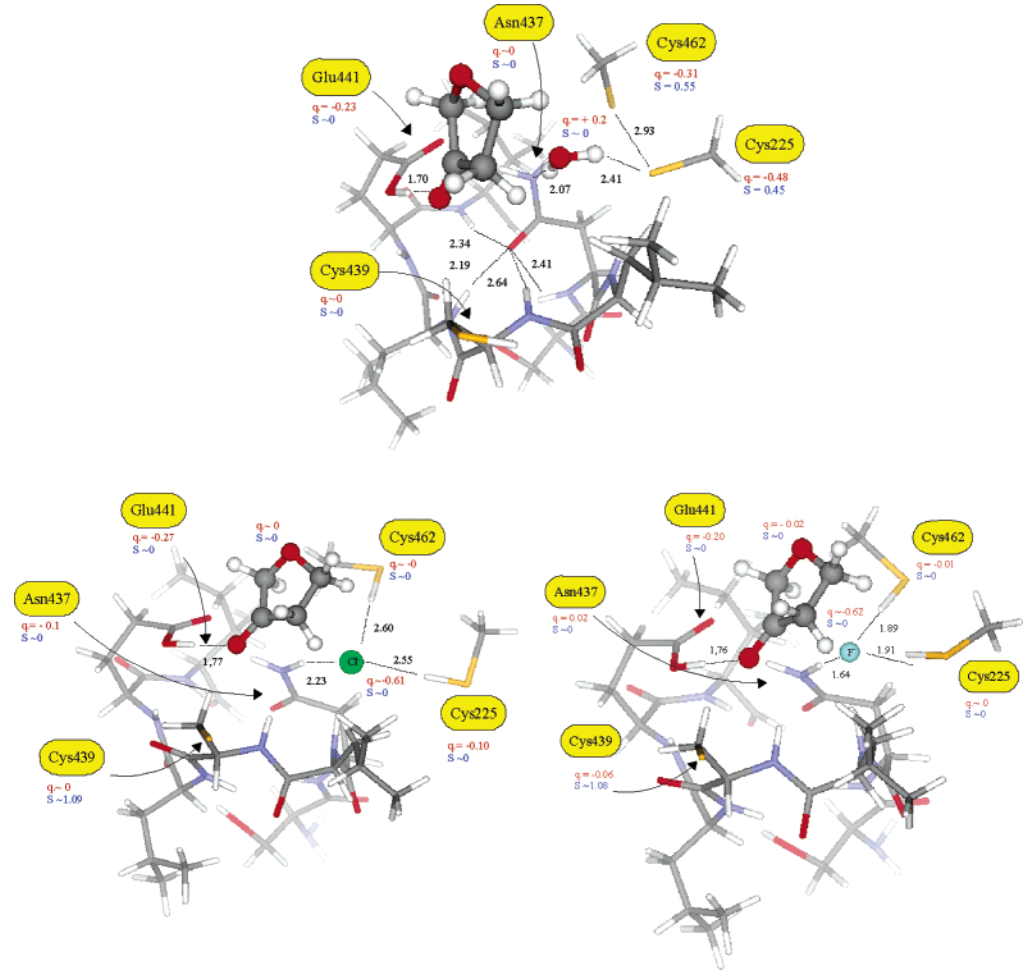

Figure 3. Calculated minima that correspond to the products of the third step of the mechanism of the natural substrate (top), CldNDP (left), and FdNDP (right). Relevant atomic charges and spin densities are included in atomic units. The substrate and the Lg group are depicted in ball-and-sticks and the enzyme in sticks.

reaction. The atoms described at the low level of theory do not suffer significant geometric modifications during the reduction pathway but are still important for the correct alignment of the active site residues.

There is a subtle difference between the terms layer and region. We have used "region" to separate the full model of the enzyme in different reactive parts, e.g., as mentioned previously, the overall system was divided into the enzyme, substrate, and Lg regions. We use "layer" to specify a set of atoms that were treated with a certain theoretical level during geometry optimization, e.g., the high-level layer contains atoms from the substrate, enzyme, and Lg regions.

The geometry of the high-level layer was optimized at a higher theoretical level, with density functional theory (DFT). The B3LYP functional was chosen, since it is known to give very good results for organic molecules. The 6-31G(d) basis set was employed, as implemented in *Gaussian 03*.[58] The inclusion of diffusion functions in the basis set for geometry optimizations has been investigated before.[59] The conclusion was that the corrections to the geometry were very small, and consequent corrections in energy differences (such as energy barriers or energies of reaction) were negligible. Therefore, it seems irrelevant from a computational point of view to include diffuse functions in geometry optimizations, considering the inherent increase in computing time that diffuse functions would cause. The low-level layer was treated with the semiempirical Austin model (AM1).[60]

The starting point of all structures used in this work was based on the products of the second step of the catalytic mechanism that has been published elsewhere,[26] i.e., immediately after the elimination of the water molecule. This minimum was obtained following the reaction coordinate that connects the respective reactants, transition states (TSs), and products through an internal reaction coordinate (IRC) calculation. The product of this step was used as the starting point to this study, and all necessary modifications were performed in order to build the desired models. In the case of the inhibitors, this means the substitutions of the water molecule by the corresponding halogen. To stabilize each system, a tight optimization was accomplished. Once all structures were stabilized, a first structure of the transition state for the elimination of the halogens was modeled and subsequently geometry-optimized toward the corresponding saddle point. To obtain the desired minima, we have indeed followed the reaction coordinate through an IRC calculation in the direction of the products, in each system. Since ONIOM calculations stops when the potential energy surface of the IRC calculation becomes slightly flat, we have reoptimized the final structures with a tighter criteria, until standard Gaussian convergence criteria were obtained.

All the minima were achieved with standard convergence criteria (Figure 3). Energy calculations were further performed by treating the whole system at the B3LYP level of theory with the 6-31+G(d) basis set. Unrestricted open-shell wave functions were used in all calculations. Spin contamination is a usual

problem in open-shell systems. We have always monitored the expectation value for S^2, and it was always lower than 0.7570, before the annihilation process. After annihilation, the S^2 expectation value was returned to the desired value of 0.7500. Atomic charges and spin densities were calculated using a Mulliken population analysis.

C. Dissociation Energy Calculations. Higher theoretical levels were used to obtain the final energies. For this purpose, the enzyme region, the substrate region, and the Lg group were taken together, and the energy of this large system was recalculated at the unrestricted DFT level of theory, with the same functional (B3LYP) and the 6-31+G(d) basis set as implemented in *Gaussian 03*.

The entropic effects were not included, because our earlier extensive experience on this system has shown us that they are very small (usually lower than 1−2 kcal/mol)[25,26,42,44−47,61] and very difficult and extremely time-consuming to calculate (namely, the frequency calculations for systems up to 100 atoms). As we are more interested in comparing the three situations (substrate, *Cl*NDP, and *F*NDP), the differential effect of entropy should be probably even smaller and will not change the conclusions derived from this work.

To simulate the enzyme and solution environments, a conductorlike polarized continuum model (CPCM) was used,[62,63] and the final energies of each model were corrected. This model accounts for the polarization of the electronic density of the solute by the solvent, and vice-versa, and is the usual choice to obtain high-level free energies of solvation with quantum mechanical systems.[23,25,26,42,44,47] It presents the advantage of allowing a self-consistent solvent−solute polarization, and recent works have estimated the accuracy of this method in 0.7 kcal/mol for neutral solutes and 1.1 kcal/mol for charged solutes.[63]

Accordingly, all models that include the enzyme, i.e., the E:S:Lg, E:S, E, and E:Lg were embedded in a dielectric continuum with a dielectric constant of 4, to simulate the enzyme environment. A dielectric constant of 4 has been shown before to produce theoretical results that are in agreement with experimental results, taking care of the protein ($e = 3$) and the buried waters environments ($e = 80$).[22,25,63] In a recent work, it was shown that the difference between a model that includes explicitly the whole R1 monomer at the QM/MM level (12 000 atoms) and a smaller model of the size of the present one, embedded in a dielectric medium with eps = 4, is less than 1 kcal/mol, for either the activation energy or the reaction energy.[26] When the substrate dissociates to solution, we have calculated its solvation energy using the same CPCM model but now with the dielectric constant of water (eps = 80). This approach has been shown to give good agreement with experimental work. In the case of the Lg groups, we have used experimental values, which were available for these species and are considered to be more accurate than the experimental ones. The hydration enthalpy values of chloride and fluoride are −364 and −506 kJ/mol, respectively. The hydration enthalpy of water is −44.02 kJ/mol. These values can be easily obtained in any physical chemistry book,[64] and to obtain the energy of the Lg groups in solution, we only need to add the respective energies in the gas phase. This energy can be easily calculated using theoretical methods (the energy of each Lg group was calculated with the same theoretical level as before).

For the sake of comparison of the results, the energies of the substrate region and the Lg group were corrected in the same way in the case of either the natural substrate or the inhibitors.

The dissociation energy calculations between the modeled enzyme for the keto-deoxyribonucleotides and the Lg group were made according to Scheme 3. In this scheme, E corresponds to the enzyme region , S is the substrate region, and Lg the leaving group. The overall complex is represented as E:S:Lg. The complex E:S+Lg contains the substrate (the keto-deoxyribonucleotide) bonded to the enzyme but without the Lg group. The complex E:Lg+S represents the complex where the substrate is dissociated from the active site but the Lg group still remains inside the active site.

SCHEME 3: Thermodynamic Scheme Used for Calculation of the Dissociation Energies

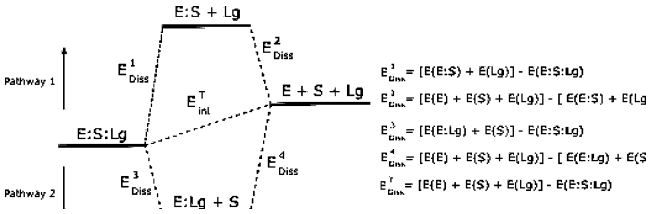

To evaluate the role of the Lg group, in the dissociation of the keto-deoxyribonucleotide from the active site, we have created two different possible pathways from which result the complete dissociation of the Lg group and the keto-deoxyribonucleotide. In pathway 1, the Lg group dissociates from the active site to the solution before the keto-deoxyribonucleotide. In pathway 2, we have built the reverse reaction, i.e., the Lg group dissociates from the active site only after the keto-deoxyribonucleotide dissociates into the solution. We emphasize that the steric arrangement of the active site allows for the dissociation to occur via the two pathways.

For simplicity of presentation in all tables and figures in which the S letter turns up, it should be read as the substrate for the natural substrate but also as the inhibitor whenever it is under their heading.

Discussion

Our first task concerned the search for the inhibitors with the closest mechanism to that of the natural substrate and with a similar active site topology after the formation of the keto-deoxyribonucleotide. With these characteristics taken into account (Scheme 2: R^2 = H) and considering the proposed inhibitory mechanisms of several inhibitors (Table 1), *Cl*dNDP and *F*dNDP were the chosen ones, since they were the most appropriate.

We shall briefly compare the complete catalytic and inhibitory mechanisms both for *F*dNDP and for *Cl*NDP (Scheme 4) as they are of prime importance for the discussion.

As it is common within most of the 2′-substrate analogues, the first and second steps of the inhibitory and normal reduction pathways are very similar. The first step involves a hydrogen atom abstraction from carbon C-3′ of the substrate by the radical Cys439. The second step is also very similar and involves a proton transfer from the hydroxyl group that is attached to carbon C-3′ of the substrate, to Glu441. At the same time, there is a concomitant dissociation of the group that is attached to carbon C-2′ of the substrate that is in close contact with the protonated Cys225. As a result, in the normal reduction pathway, a radical keto-ribonucleotide and a water molecule are obtained; Cys225 becomes anionic and in close contact with the protonated Cys462. In the inhibitory process, the same radical keto-ribonucleotide is produced, and the dissociation of both halogens from the ribose ring also takes place. However, in this case due to the pK_a of the leaving groups (HF = 3.16 and HCl = 7), they do not become protonated, and Cys225 remains protonated.

SCHEME 4: Reduction Mechanism of the Natural Substrate and of the 2′-Halogen Substrate Analogue Mechanism (i.e., CldNDP and FdNDP)

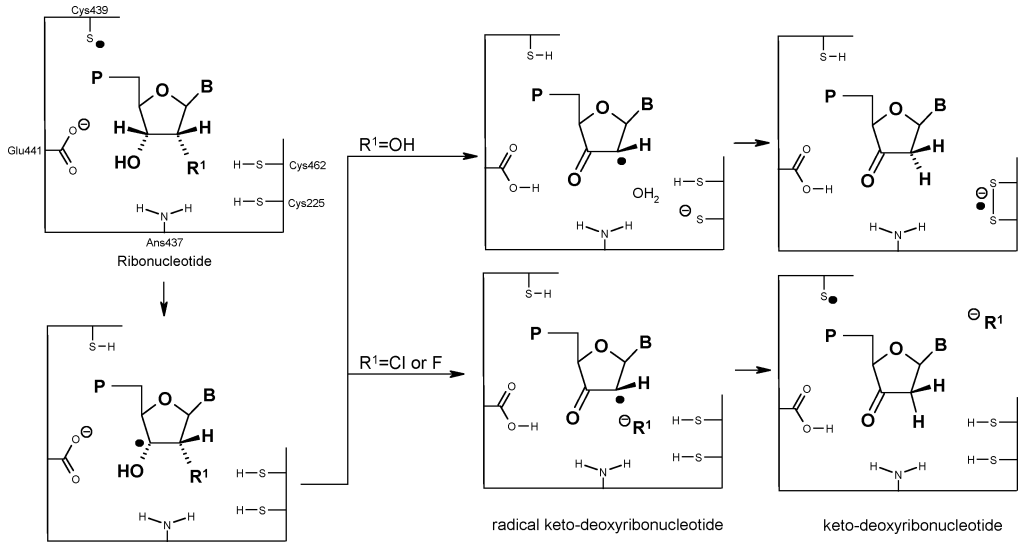

TABLE 2: Interactions between the Active Site Residues, the Substrate, and the Leaving Group[a]

	O(E441)−O(C-3′)	O(E441)−H(N437)	H(N437)−S(C462)	S(C225)-S(C462)	X−S(C462)	X−S(C225)	X−N(N437)	X−C−2′(furanone)
natural substrate X = H_2O	1.7	2.0	2.3	2.9		2.4	2.1	2.6
*F*dNDP X = F	1.8	2.1		4.4	1.9	1.9	1.6	2.6
*Cl*dNDP X = Cl	1.8	2.1		4.9	2.6	2.6	2.2	2.9

[a] The name of the amino acid and the corresponding number are given in parentheses.

In the third step of the normal reduction pathway, there is a proton transfer from Cys462 to Cys225, after which there is a hydrogen atom transfer from Cys225 to carbon C-2′ of the ribose ring. This step is assisted by a water molecule that behaves as a hydrogen splitter, helping the migration of the hydogren atom. As products of this step, we find Cys225 and Cys462 linked by a radical anionic disulfide bridge and the keto-deoxyribonucleotide inside the active site. In the case of the inhibitors, the anionic halogen interacts with both hydrogen atoms of Cys225 and Cys462, precluding the hydrogen atom transfer to carbon C-2′ of the substrate.

It is known from experimental work[65−67] that both inhibitors give rise to a keto-deoxyribonucleotide that will dissociate from the active site and, in solution, will generate the respective furanone derivative. Moreover, it was detected by UV spectroscopy that at the end of this step, and in the presence of reductors, the tyrosyl radical is regenerated, contrary to what happens with the natural substrate. These clues, associated with the proposed mechanisms, point to a hydrogen atom transfer from Cys439 to carbon C-2′ of the substrate. The only thing that can be questioned is if there is any kind of constraint in the mobility of Cys439 that could preclude this reaction. The optimizations with the extended model of the active site, performed before, have shown that, after the second step, Cys439 is very close to the carbon C-2′ of the substrate, and therefore, there is no steric constraint that can prevent the hydrogen atom transfer to the carbon C-2′ of the substrate.[26]

In summary, in the products of all three cases under study, a keto-deoxyribonucleotide is inside the active site but within different environments. While in the natural substrate, Cys225 and Cys462 are linked by a radical anionic dissulfide bridge and Cys439 remains protonated, in both cases of *F*dNDP and *Cl*dNDP, the charge is concentrated in the anionic halogens, and Cys439 is found as a radical.

To evaluate why the ketone leaves the active site during the inhibition mechanism as opposed to what happens with the natural substrate, we have created three systems, corresponding to the products of the fourth/third step of each case. All models contain 140 atoms and include the substrate (the furanone), a heptapeptide that links all residues from Ile436 to Leu442, and Cys225 and Cy2462 as free residues. The heptapetide constrains the movement of important active site residues, i.e., Cys439, Glu441, and Asn437, providing a better description of the active site.

The mechanisms of our systems have already been extensively studied elsewhere.[4,23−26] and therefore, we did not follow the mechanism of each modeled system until the formation of the keto-deoxyribonucleotide. Instead, the starting point of this paper was the product of the second step of the normal pathway. Depending on the modeled system, the leaving group was changed to a water molecule, an anionic fluoride, or anionic chlorine, and the substrate was modified to a keto-deoxyribonucleotide. As the protonation and the hybridization states of Cys225, Cys439, and Glu441 change depending on the modeled reaction and as the Lg group is free to move inside the active site, all minima were obtained after refined scans with a reaction coordinate which followed the products of the second step of the normal pathway to the formation of the keto-deoxyribonucleotide.

Once all minima were obtained with standard convergence criteria and without any imaginary frequency, it was clear that the network of hydrogen bonds was different between all models, regarding the active site and the substrate regions and the Lg group (Table 2).

In the model with the natural substrate, the ketone group bonded to C-3′ of the substrate makes only one hydrogen bond with the protonated oxygen from Glu441 (1.7 Å). The rest of the hydrogen bonds are centered in Asn437, making a net of

SCHEME 5: Thermodynamic Pathways that Induce the Dissociation of the Keto-Deoxyribonucleotide and the Lg Group into the Solution in the Natural Substrate, the ClNDP, and the FdNDP

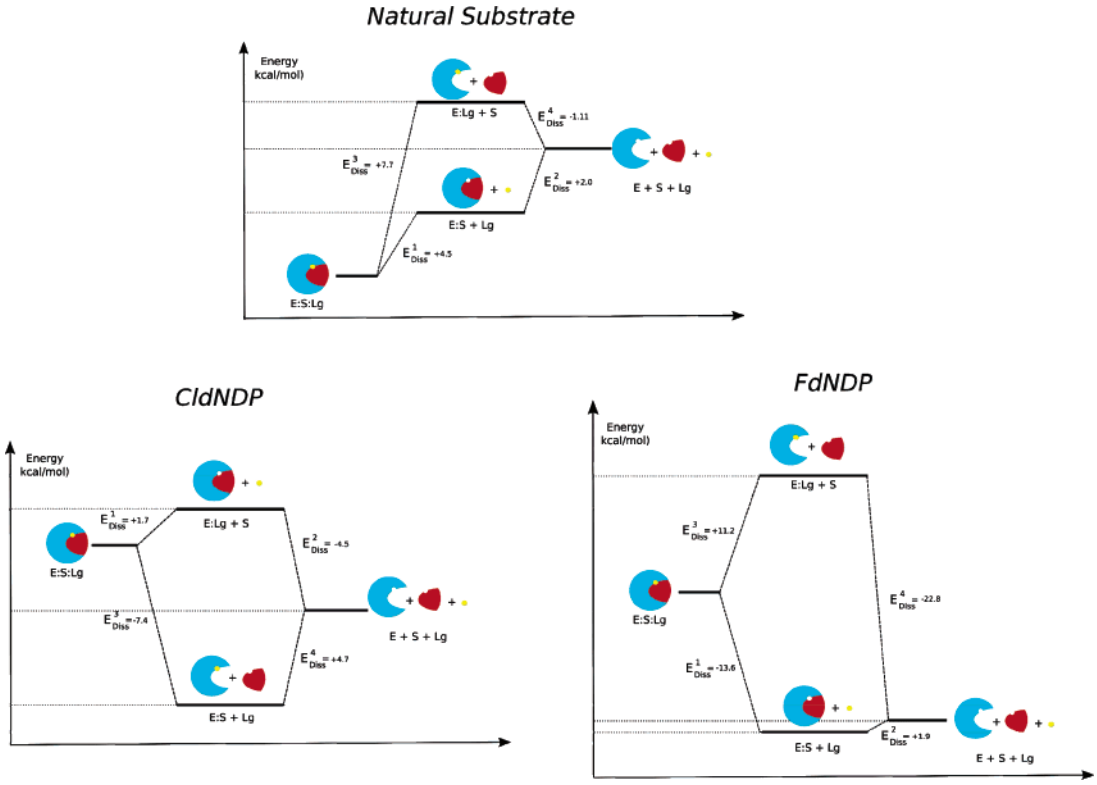

hydrogen bonds around the substrate: one of the hydrogens from the amide group of Asn437 makes a hydrogen bond with Glu441 (2.0 Å), and the other with Cys462 (2.3 Å). The water molecule released after the second step and believed to be important in the third step remains between the substrate (2.6 Å) and Cys225 (2.4 Å) and makes a hydrogen bond with the nitrogen from the amide group of Asn437 (2.1 Å). It is also clear that the carbonyl group of the amide of As437 is important, since it maintains the cohesion of the active site by making several hydrogen bonds with several NH groups of the heptapeptide chain. Besides these interactions, the model predicts that both cysteines become closer by 2.9 Å, with the charge (−0.80 au) and spin (0.99 au) concentrated on them, correctly generating the experimentally observed radical anionic disulfide bridge.

In the case of *F*dNDP and *Cl*dNDP, the networks of hydrogen bonds are quite different as a consequence of the reorientation of Asn437. In comparison with the natural substrate, the only similarities are the hydrogen bonds that involve the protonated Glu441 and the ketone of the substrate (∼1.7 Å) and the hydrogen from the amide group of Asn437 (∼2.1 Å). The other hydrogen bonds are centered in the anionic halogen, instead of Asn437, to stabilize the negative charge. From these, it is clear to notice the interaction between the anions with the hydrogen from the amide group of Asn437 (1.6 Å in the case of the fluoride and 2.2 Å with the chlorine) and with each hydrogen from Cys225 (1.9 Å in the case of the anionic fluoride and 2.6 Å in the chlorine) and Cys462 (1.9 Å in the case of the fluoride and 2.6 Å in the chlorine). The cysteines are now separated by 4.3 Å in the case of the fluorine and 4.9 Å in the case of the chlorine. Due to the hydrogen atom transfer between Cys439 and carbon C-2′ from the substrate, the spin is now concentrated at Cys439 (1.08 au in *F*dNDP and 1.10 au in *Cl*dNDP), instead of Cys225, as with the natural substrate thus precluding the formation of the anionic radical disulfide bridge in the case of the analogues.

The observed net of hydrogen bonds and charge dispersion of each model show that the active site of the natural substrate is the most stable, contrary to what happens with the inhibitors in which the net of hydrogen bonds and the charge are concentrated in the anions. This can be viewed as a consequence of (i) the Asn437 orientation that allows an increase in the network of hydrogen bonds between the residues of the active site resulting in a better stabilization of the complex and (ii) the extended charge dispersion between Glu441 Cys225 and Cys462 that also stabilizes the system, and can be viewed as a consequence of the close interaction between several residues of the active site promoted by the water molecule.

However, and since we are handling different minima, the total energy of each system cannot give us any ideas about the stability of the complexes. To obtain the correct meaning, we have calculated dissociation energies. As the active site topology is somewhat similar in all systems, we have also investigated the influence of the Lg group in the calculated dissociation energies. There are two possible pathways from which may result the dissociation of the keto-deoxyribonucleotide and of the Lg group from the active site. The first pathway simulates the dissociation of the keto-deoxyribonucleotide from the active site before the dissociation of the Lg group takes place. The second pathway simulates the reverse scenery, i.e., the dissociation of the Lg group before the dissociation of the keto-deoxyribonucleotide from the active site. The calculated dissociation energies that result from each pathway can be seen in Table 3 and schematically in Scheme 5.

The calculated dissociation energies $E_{Diss}{}^{T}$ in Table 3 confirm all the observations made previously and demonstrate that, due to the active site topology, the keto-deoxyribonucleotide and the leaving group have a much lower tendency to dissociate in the case of the substrate than that of the inhibitors. In fact, the number of hydrogen bonds and the charge/spin delocalization between the active site and the keto-deoxyribonucleotide are

TABLE 3: Dissociation Energies for Each Model with Meanings Associated to Scheme 3

	dissociation energies				
system	E_{Diss}^1	E_{Diss}^2	E_{Diss}^3	E_{Diss}^4	$E_{Diss}^T = E_{Diss}^1 + E_{Diss}^2 = E_{Diss}^3 + E_{Diss}^4$
natural substrate	4.5	2.0	7.7	−1.1	6.5
*Cl*dNDP	1.7	−4.5	−7.4	4.7	−2.8
*F*dNDP	−13.6	1.9	11.2	−22.8	−11.7

more feasible for a better binding in the case of the normal substrate than in the case of the substrate analogues. The water molecule seems therefore to have a crucial role in the normal reduction pathway in this step, allowing a better cohesion and stability of the complex. These results match the experimental observations where the anionic halogens plus the furanone derivative are detected in solution in the case of the substrate analogues, contrary to what happens with the substrate.

The results show that, independently of the followed pathway, in the normal reduction mechanism the dissociation of the substrate and the leaving group from the active site into the solution is thermodynamically unfavorable by ~7 kcal/mol.

However, with the case of the inhibitors the situation is different. In both cases and independent of the pathway, the unbound complex has always a lower energy than the bonded complex, contrary to what happens to the natural substrate. Therefore, in the latter cases, there is a dissociation of the Lg group and the keto-deoxyribonucleotide into the solution, as has been observed experimentally.

The pathways followed by *Cl*dNDP and *F*dNDP are however somewhat different. In *Cl*dNDP, the dissociation of the inhibitor from the complex is very favorable and occurs prior to the less favorable release of Cl^- into the solution. As for the *F*dNDP, the release of F^- is very favorable but occurs before the dissociation of the inhibitor. Although the dissociation of the inhibitor in *F*dNDP and the dissociation of Cl^- in *Cl*dNDP are slightly unfavored thermodynamically, this does not mean that they do not occur, as the entropic contributions are not included in the dissociation energy. These contributions will favor the dissociated state. Moreover, the theoretical method itself has an accuracy of about 3 kcal/mol; therefore, what is really meaningful here are the trends between the natural substrate and the inhibitors, and between both inhibitors, and not the absolute energy values, which are very close to zero and affected by an uncertainty which is not insignificant. Relative energies, deriving from comparison of the natural substrate and the inhibitors are much less affected by systematic errors, and consequently much more accurate. In this context, we conclude that (i) the natural substrate and the water molecule are indeed more tightly bound than any of the inhibitors, which makes meaningful the hypothesis that the catalytic pathway can proceed according to the earlier proposal depicted in Scheme, 2 (ii) the inhibitors are indeed weakly bound to the active site, allowing their dissociation and enzyme inhibition, in agreement with the inhibition mechanism depicted in Scheme 2, and (iii) the F^- ion has a better ability to dissociate from the active site, compared to Cl^-, contrary to the inhibitor itself, in which case it dissociates better in the case of CldNDP.

The calculated dissociation energies (E_{Diss}^T) in each pathway and the consequent dissociation of the keto-deoxyribonucleotide into solution, within both inhibitors, alerts for the low stability of the complex composed by the enzyme and the keto-deoxyribonucleotide, whenever the Lg group is in solution or inside the active site. This can be explained by taking in account (i) the presence of the anion inside the active site that prevents the stabilization of the complex enzyme/substrate, because it centers in itself the network of the hydrogen bonds, and (ii) when the anion is in solution, the loss of the active site electrostatics due to the charge transfer to the solvent.

The apparent stability of the Cl^- inside the active site shows that the anion is better stabilized inside the enzyme rather than in solution. This occurs due to the network of charged hydrogen bonds promoted by Cys255, Cys462, and Asn437. It is interesting to note that this stabilization overcomes the solvation free energy of the anion. In the case of the *F*dNDP, the preferential stabilization of the anion inside the active site is not observed, and the anion dissociation is always favored in both pathways. These facts show that the stabilization provided by the active site, although larger than in the case of Cl^-, does not compensate the very favorable solvation free energy of F^-, contrary to what happens with *Cl*dNDP.

It is interesting to observe that in the case of *F*dNDP the dissociation of the keto-deoxyribonucleotide, in both pathways, always leads to higher-energy states, compared to what happens with *Cl*dNDP. Moreover, the dissociation of the keto-deoxyribonucleotde when the Lg group is inside the active site requires 11.2 kcal/mol (E_{diss}^3), which is much higher than 1.9 kcal/mol (E_{diss}^2) when the keto-deoxyribonucleotide is the only species inside the active site. This means that, with *F*dNDP, the presence of the anion inside the active site allows a better stabilization of the keto-deoxyribonucleotide, slowing down its dissociation into solution.

The experimental study of 2′-halogen inhibitors, performed by Stubbe et al. in 1987[68] besides the enzyme inactivation by furanone derivatives, reveals that even though the inhibition is independent of the stereochemistry of the 2′-substituent, the partitioning between normal and abnormal turnover varies predictably with the 2′ substituent leaving group ability and reaction pH. The experimental work shows that with 2′-Cl ($pK_a = -7$) and 2′-F ($pK_a = 3.2$) the enzyme is inhibited, and the formation of the furanone derivative and the anions are detected in solution. In the case of *Cl*dNDP, the abnormal 4 formation predominates over normal reduction, and the Cl^- ion is stoichiometrically released into solution when (and only when) the enzyme is inhibited. However, in the case of *F*dNDP, normal reduction predominates over abnormal ketone formation, and the F^- ion is always released into solution regardless of which pathway (turnover/inhibition) is followed.

Our results are fully coherent with these experimental observations. The theoretical calculations do predict that the fluorine ion will always be released, independently of the release of the inhibitor. Therefore, the full dissociation of F^- should be expected. In the case of Cl^-, the preferred pathway involves the dissociation of the inhibitor prior to the ion, which is consistent with the release of the ion proportionally to the amount of enzyme inhibited.

Conclusions

Inhibition of the nucleotide biosynthesis in tumor cells by antimetabolites is a classic yet important approach in cancer chemotherapy. The obtained results point out that the inhibitory mechanisms related with the favorable dissociation of the 2′-group promote the dissociation of the keto-deoxyribonucleotide into the solution. Once in solution, this keto-deoxyribonucleotide is responsible for the formation of a furanone derivative that inactivates the enzyme.

The results demonstrate that the main cause for the dissociation of the keto-deoxyribonucleotide is dependent on very favorable free energies of solvation of the leaving groups and

the reorganization of the hydrogen bonds around them inside the active site. In the substrate reduction pathway, the presence of the neutral water molecule with a weak energy of solvation stabilizes the hydrogen-bonding network that promotes the stability of the active site complex precluding the dissociation of the keto-deoxyribonucleotide. In the case of the inhibitors, the presence of anions inside the active site prevents the stabilization of the enzyme/substrate complex by centering itself in the hydrogen bond network and, when the anion is in solution, by the loss of the active site electrostatics due to the charge transfer from the protein hydrophobic active site to the water environment.

We have also shown that the fluorine ion dissociates prior to the inhibitor, contrary to what happens with the chlorine ion. These results are consistent with the experimental observations of the different extents of dissociation of the ions in the two cases.

The water molecule as in previous steps has a preponderant role in the substrate reduction pathway mechanism. As has been shown before,[23] it can be viewed as a reactive molecule that can function as a hydrogen splitter in the third step of the substrate reduction pathway, and in this step, it is essential for the stability of the active site complex and allows for a better interaction between the enzyme and the substrate.

References and Notes

(1) Reichard, P. *Science* **1993**, *260*, 1773.
(2) Stubbe, J. A. *J. Biol. Chem.* **1990**, *265*, 5329.
(3) Sjoberg, B. M.; Graslund, A. *Adv. Inorg. Biochem.* **1983**, *5*, 87.
(4) Cerqueira, N. M. F. S. A.; Pereira, S.; Fernandes, P. A.; Ramos, M. J. *Curr. Med. Chem.* **2005**, *12*, 1283.
(5) vanderDonk, W.; Licht, S.; daSalva, D.; McCarthy, J.; Robins, M. J.; Stubbe, J. *FASEB J.* **1996**, *10*, 503.
(6) Sjoberg, B. M. *Met. Sites Proteins Models: Ion Cent., 1997* **1997**, *88*, 139.
(7) Stubbe, J.; Ackles, D.; Segal, R.; Blakley, R. L. *J. Biol. Chem.* **1981**, *256*, 4843.
(8) Stubbe, J.; Ge, J.; Yee, C. S. *Trends Biochem. Sci.* **2001**, *26*, 93.
(9) Sjoberg, B. M. *Structure* **1994**, *2*, 793.
(10) vanderDonk, W. A.; Yu, G. X.; Silva, D. J.; Stubbe, J. *Biochemistry* **1996**, *35*, 8381.
(11) Kashlan, O. B.; Scott, C. P.; Lear, J. D.; Cooperman, B. S. *Biochemistry* **2002**, *41*, 462.
(12) Kashlan, O. B.; Cooperman, B. S. *Biochemistry* **2003**, *42*, 1696.
(13) Persson, A. L.; Eriksson, M.; Katterle, B.; Potsch, S.; Sahlin, M.; Sjoberg, B. M. *J. Biol. Chem.* **1997**, *272*, 31533.
(14) Johnston, M. I.; Mao, S. S.; Bollinger, J. M.; Stubbe, J. *Biochemistry* **1989**, *28*, 1939.
(15) Kasrayan, A.; Persson, A. L.; Sahlin, M.; Sjoberg, B. M. *J. Biol. Chem.* **2002**, *277*, 5749.
(16) Bollinger, J. M.; Krebs, C.; Vicol, A.; Chen, S. X.; Ley, B. A.; Edmondson, D. E.; Huynh, B. H. *J. Am. Chem. Soc.* **1998**, *120*, 1094.
(17) Stubbe, J.; Yee, C. S.; Chang, M. C. Y.; Ge, J.; Nocera, D. G. *Abstr. Pap. Am. Chem. Soc.* **2003**, *226*, U158.
(18) Lawrence, C. C.; Bennati, M.; Obias, H. V.; Bar, G.; Griffin, R. G.; Stubbe, J. *Proc. Natl. Acad. Sci. U.S.A.* **1999**, *96*, 8979.
(19) van der Donk, W. A.; Yu, G. X.; Perez, L.; Sanchez, R. J.; Stubbe, J.; Samano, V.; Robins, M. J. *Biochemistry* **1998**, *37*, 6419.
(20) Mohr, M.; Zipse, H. *Chem.—Eur. J.* **1999**, *5*, 3046.
(21) Zipse, H. *Org. Biomol. Chem.* **2003**, *1*, 692.
(22) Siegbahn, P. E. M. *J. Am. Chem. Soc.* **1998**, *120*, 8417.
(23) Cerqueira, N. M. F. S. A.; Fernandes, P. A.; Ramos, M. J.; Eriksson, L. A. *THEOCHEM* **2004**, *53*, 53.
(24) Pelmenschikov, V.; Cho, K. B.; Siegbahn, P. E. *J. Comput. Chem.* **2004**, *25*, 311.
(25) Cerqueira, N. M. F. S. A.; Fernandes, P. A.; Ramos, M. J.; Eriksson, L. A. *J. Comput. Chem.* **2004**, *25*, 2031.
(26) Cerqueira, N. M. F. S. A.; Fernandes, P. A.; Ramos, M. J.; Eriksson, L. A. *Biophys. J.* **2006**, *90*, 2109.
(27) Baker, C. H.; Banzon, J.; Bollinger, J. M.; Stubbe, J.; Samano, V.; Robins, M. J.; Lippert, B.; Jarvi, E.; Resvick, R. *J. Med. Chem.* **1991**, *34*, 1879.
(28) Cardoen, S.; Van Den Neste, E.; Smal, C.; Rosier, J. F.; Delacauw, A.; Ferrant, A.; Van den Berghe, G.; Bontemps, F. *Clin. Cancer Res.* **2001**, *7*, 3559.
(29) Thelander, L.; Larsson, B. *J. Biol. Chem.* **1976**, *251*, 1398.
(30) Robins, M. J.; Samano, V.; Zhang, W. J.; Balzarini, J.; Declercq, E.; Borchardt, R. T.; Lee, Y.; Yuan, C. S. *J. Med. Chem.* **1992**, *35*, 2283.
(31) Stubbe, J.; Kozarich, J. W. *J. Biol. Chem.* **1980**, *255*, 5511.
(32) Stubbe, J.; Kozarich, J. W. *J. Am. Chem. Soc.* **1980**, *102*, 2505.
(33) Coves, J.; deFallois, L. L. H.; lePape, L.; Decout, J. L.; Fontecave, M. *Biochemistry* **1996**, *35*, 8595.
(34) Heinemann, V.; Xu, Y. Z.; Chubb, S.; Sen, A.; Hertel, L. W.; Grindey, G. B.; Plunkett, W. *Mol. Pharmacol.* **1990**, *38*, 567.
(35) Kanazawa, J.; Takahashi, T.; Akinaga, S.; Tamaoki, T.; Okabe, M. *Anti-Cancer Drugs* **1998**, *9*, 653.
(36) Salowe, S.; Bollinger, J. M., Jr.; Ator, M.; Stubbe, J.; McCraken, J.; Peisach, J.; Samano, M. C.; Robins, M. J. *Biochemistry* **1993**, *32*, 12749.
(37) Ashley, G. W.; Harris, G.; Stubbe, J. *Biochemistry* **1988**, *27*, 4305.
(38) Ashley, G. M.; Stubbe, J. *Biochemistry* **1988**, *27*, 3110.
(39) Sjoberg, B. M.; Graslund, A.; Eckstein, F. *J. Biol. Chem.* **1983**, *258*, 8060.
(40) Sjoberg, B. M.; Sahlin, M. *Protein Sens. React. Oxygen Species, Part B, 2002* **2002**, *348*, 1.
(41) Ator, M. A.; Stubbe, J. *Biochemistry* **1985**, *24*, 7214.
(42) Pereira, S.; Fernandes, P. A.; Ramos, M. J. *J. Am. Chem. Soc.* **2005**, *127*, 5174.
(43) Himo, F.; Siegbahn, P. E. M. *J. Phys. Chem. B* **2000**, *104*, 7502.
(44) Pereira, S.; Fernandes, P. A.; Ramos, M. J. *J. Comput. Chem.* **2004**, *25*, 227.
(45) Fernandes, P. A.; Ramos, M. J. *J. Am. Chem. Soc.* **2003**, *125*, 6311.
(46) Fernandes, P. A.; Ramos, M. J. *Chem.—Eur. J.* **2003**, *9*, 5916.
(47) Pereira, S.; Fernandes, P. A.; Ramos, M. J. *J. Comput. Chem.* **2004**, *25*, 1286.
(48) Pereira, S.; Cerqueira, N. M.; Fernandes, P. A.; Ramos, M. J. *Eur. Biophys. J.* **2006**, *35*, 125.
(49) Eriksson, M.; Uhlin, U.; Ramaswamy, S.; Ekberg, M.; Regnstrom, K.; Sjoberg, B. M.; Eklund, H. *Structure* **1997**, *5*, 1077.
(50) Uhlin, U.; Eklund, H. *Nature (London)* **1994**, *370*, 533.
(51) Nordlund, P.; Sjoberg, B. M.; Eklund, H. *Nature (London)* **1990**, *345*, 593.
(52) Insight; www.accelrys.com (accessed 2000).
(53) Bakowies, D.; Thiel, W. *J. Phys. Chem. B* **1996**, *100*, 10580.
(54) Dapprich, S.; Komaromi, I.; Byun, K. S.; Morokuma, K.; Frisch, M. J. *THEOCHEM* **1999**, *461*, 1.
(55) Sherwood, P. Hybrid Quantum Mechanics/Molecular Mechanics Approaches. In *Modern Methods and Algorithms of Quantum Chemistry*; 2000.
(56) Svensson, M.; Humbel, S.; Froese, R. D. J.; Matsubara, T.; Sieber, S.; Morokuma, K. *J. Phys. Chem.* **1996**, *100*, 19357.
(57) Torrent, M.; Vreven, T.; Musaev, D. G.; Morokuma, K.; Farkas, O.; Schlegel, H. B. *J. Am. Chem. Soc.* **2002**, *124*, 192.
(58) Frisch, M. J.; Trucks, G. W.; Schlegel, H. B.; Scuseria, G. E.; Robb, M. A.; Cheeseman, J. R.; Montgomery, J. A., Jr.; Vreven, T.; Kudin, K. N.; Burant, J. C.; Millam, J. M.; Iyengar, S. S.; Tomasi, J.; Barone, V.; Mennucci, B.; Cossi, M.; Scalmani, G.; Rega, N.; Petersson, G. A.; Nakatsuji, H.; Hada, M.; Ehara, M.; Toyota, K.; Fukuda, R.; Hasegawa, J.; Ishida, M.; Nakajima, T.; Honda, Y.; Kitao, O.; Nakai, H.; Klene, M.; Li, X.; Knox, J. E.; Hratchian, H. P.; Cross, J. B.; Bakken, V.; Adamo, C.; Jaramillo, J.; Gomperts, R.; Stratmann, R. E.; Yazyev, O.; Austin, A. J.; Cammi, R.; Pomelli, C.; Ochterski, J. W.; Ayala, P. Y.; Morokuma, K.; Voth, G. A.; Salvador, P.; Dannenberg, J. J.; Zakrzewski, V. G.; Dapprich, S.; Daniels, A. D.; Strain, M. C.; Farkas, O.; Malick, D. K.; Rabuck, A. D.; Raghavachari, K.; Foresman, J. B.; Ortiz, J. V.; Cui, Q.; Baboul, A. G.; Clifford, S.; Cioslowski, J.; Stefanov, B. B.; Liu, G.; Liashenko, A.; Piskorz, P.; Komaromi, I.; Martin, R. L.; Fox, D. J.; Keith, T.; Al-Laham, M. A.; Peng, C. Y.; Nanayakkara, A.; Challacombe, M.; Gill, P. M. W.; Johnson, B.; Chen, W.; Wong, M. W.; Gonzalez, C.; Pople, J. A. *Gaussian 03*, revision C.02; Gaussian, Inc.: Wallingford, CT, 2004.
(59) Hertwig, R. H.; Koch, W. *J. Comput. Chem.* **1995**, *16*, 576.
(60) Dewar, M. J. S.; Zoebisch, E. G.; Healy, E. F.; Stewart, J. J. P. *J. Am. Chem. Soc.* **1995**, *107*, 3902.
(61) Fernandes, P. A.; Eriksson, L. A.; Ramos, M. J. *Theor. Chem. Acc.* **2002**, *108*, 352.
(62) Barone, V.; Cossi, M. *J. Phys. Chem. A* **1998**, *102*, 1995.
(63) Cossi, M.; Rega, N.; Scalmani, G.; Barone, V. *J. Comput. Chem.* **2003**, *24*, 669.
(64) Atkins, P. W. *Physical Chemistry*, 2nd ed.; Oxford University Press: New York, 1982.
(65) Harris, G.; Ator, M.; Stubbe, J. *Biochemistry* **1984**, *23*, 5214.
(66) Stubbe, J.; Smith, G.; Blakley, R. L. *J. Biol. Chem.* **1983**, *258*, 1619.
(67) Stubbe, J.; Ator, M.; Krenitsky, T. *J. Biol. Chem.* **1983**, *258*, 1625.
(68) Harris, G.; Ashley, G. W.; Robins, M. J.; Tolman, R. L.; Stubbe, J. *Biochemistry* **1987**, *26*, 1895.